Available online at www.sciencedirect.com
ScienceDirect
Journal of the European Ceramic Society 31 (2011) 2377–2385
www.elsevier.com/locate/jeurceramsoc

Synthesis of zirconium oxycarbide (ZrC_xO_y) powders: Influence of stoichiometry on densification kinetics during spark plasma sintering and on mechanical properties

Mathieu Gendre *, Alexandre Maître, Gilles Trolliard

Laboratoire Science des Procédés Céramiques et Traitements de Surface, UMR CNRS 6638, Centre Européen de la Céramique, 12, rue Atlantis, 87068 Limoges Cedex, France

Received 20 December 2010; received in revised form 17 May 2011; accepted 25 May 2011
Available online 21 June 2011

Abstract

Different stoichiometries of zirconium oxycarbide (ZrC_xO_y) powders were synthesised by carboreduction to approach the role of the chemical composition on the densification behaviour during spark plasma sintering and on the mechanical properties. Chemical analyses were performed using complementary methods to determine the actual stoichiometry and homogeneity of powders. Evolution of relative density during SPS treatment and microstructure observations by SEM showed that oxygen and vacancy contents would enhance the densification kinetics by promoting the lattice diffusion of limiting species. A study of mechanical properties of SPS sintered specimens has highlighted their significant dependence on the oxycarbide stoichiometry, especially at high temperature.
© 2011 Elsevier Ltd. All rights reserved.

Keywords: Zirconium (oxy)carbide; Spark plasma sintering; Chemical properties; Mechanical properties; Electron microscopy

1. Introduction

The transition metal carbides (*e.g.* ZrC and TiC) show promising thermomechanical properties at high temperature such as elastic properties, creep and corrosion resistance.[1] Consequently, these refractory materials could be used as structural material for furnace elements or as plasma arc electrodes. Moreover, ZrC-based materials are also candidates as fuels shielding materials for future nuclear reactors.[2] However, due to the high melting temperature of the carbides, their sintering requires high applied load and temperature[3] and/or the use of sintering aids.[4–6] As a consequence, nonconventional sintering methods, such as spark plasma sintering (SPS), can be used in order to reach full dense samples.[5,7,8] Indeed, this method allows enhancing the densification kinetics and, consequently, decreases the sintering time.[9] Finally, the SPS method would lead to finer microstructures than those reached by hot-pressing method and thus better mechanical properties.

The most common route to synthesize zirconium carbide consists in carburizing the zirconium oxide (ZrO_2) according to the following equation:

$$ZrO_{2(s)} + 3C_{(s)} \rightarrow ZrC_{(s)} + 2CO_{(g)} \quad (1)$$

However, this method can lead to the presence of residual oxygen in the carbide lattice, resulting in the stabilization of a zirconium oxycarbide composition ZrC_xO_y. Both structural and kinetic factors can explain the presence of this oxycarbide phase after carboreduction. First, it is well known that the zirconium carbide ZrC_x could admit a wide range of non-stoichiometry (x) in carbon. In particular, (x) coefficient may range between 0.6 and 0.98.[10–13] As a consequence, oxygen atoms could occupy a carbon vacancy or replace carbon atoms to form an oxycarbide phase ZrC_xO_y.[14–16] Therefore, residual free carbon is an impurity usually detected after reaction (1) because of a non-homogeneous reaction or because of the non-stoichiometry of the zirconium carbide phase.[11–16]

The aim of this work is twofold: (i) to synthesize zirconium oxycarbide powders with controlled stoichiometry (*i.e.* carbon and oxygen contents) and microstructure (*i.e.* micro-sized grains); (ii) to study the influence of the stoichiometry on

* Corresponding author. Tel.: +33 5 87 50 23 70.
E-mail address: mathieu.gendre@unilim.fr (M. Gendre).

0955-2219/$ – see front matter © 2011 Elsevier Ltd. All rights reserved.
doi:10.1016/j.jeurceramsoc.2011.05.037

the densification behaviour of oxycarbide compacts during spark plasma sintering and, finally, on their mechanical properties.

2. Experimental procedure

2.1. Synthesis of oxycarbide powders

The carboreduction route[17] has been employed to synthesise zirconium oxycarbide powders from commercially available carbon (amorphous carbon black, 99.25%, Prolabo, France) and zirconia powders (monoclinic, 99.5%, Alfa Aesar, Germany). The theoretical equation (1) has been modified to reach the desired theoretical stoichiometry of oxycarbide, with $x = C/Zr$ and $y = O/Zr$:

$$ZrO_{2(s)} + (2 + x - y)C_{(s)} \rightarrow ZrC_xO_{y(s)} + (2 - y)CO_{(g)} \quad (2)$$

Then, the sum of the two ratios $x = C/Zr$ and $y = O/Zr$ has been fixed to be equal to 1. In a first approach, that means no carbon vacancy remains in the zirconium oxycarbide lattice which is completely saturated. Under this hypothesis, the reaction of the zirconia carboreduction can be expressed as follows:

$$ZrO_{2(s)} + (1 + 2x)C_{(s)} \rightarrow ZrC_xO_{1-x(s)} + (1 + x)CO_{(g)} \quad (3)$$

The coefficient x ($x = C/Zr$, $1 - x = O/Zr$) has been fixed to reach different zirconium oxycarbide stoichiometries. Seven values for x (respectively $1 - x$) have been retained: 1.00 (0.00), 0.95 (0.05), 0.90 (0.10), 0.80 (0.20), 0.70 (0.30), 0.60 (0.40) and 0.50 (0.50).

Carbon and zirconia initial powders were mixed in previously fixed stoichiometric proportions using a low speed planetary ball mill. The blending sequence was composed of 5 pulses of 1 min at 200 rpm interrupted by pauses of 2 min to prevent heating. Each mixture was then treated at 2023 K for 8 h in a graphite furnace (V.A.S. furnace, Suresnes, France) under flowing argon (30 L h^{-1}). Finally, powders were sieved in dry way (40 μm) to remove the partially unreacted zirconia agglomerates present after thermal treatment and whose average size largely exceeds 40 μm. It must be noticed that this residual content of zirconia agglomerates remains inferior to 0.2 wt.% as reported in a previous study.[18]

2.2. Spark plasma sintering of powders

SPS treatments (SPS-2080, Syntec Inc., Kanagawa, Japan) have been performed thanks to the PNF[2] platform (University of Toulouse, France). These attempts were achieved under vacuum, using a 20 mm diameter graphite die lined with graphite paper (Papyex®, Carbone Lorraine, Genevilliers, France). The heating rate was fixed to 100 K/min up to the targeted temperature. The latter temperature was corrected according to the procedure reported in a previous work.[19] Finally, in order to get the instantaneous value of the relative density of samples, the actual displacement variation of the pistons have been corrected for each thermal cycle, taking into account the thermal expansion of graphite parts.

2.3. Characterization of samples

The global analysis of oxygen and carbon content was achieved by elemental chemical analysis using combustion analysers: EMGA 600W (Horiba, Kyoto, Japan) for carbon and EMIA 221V (Horiba, Kyoto, Japan) for oxygen. Each apparatus uses the quantification of the $CO_{2(g)}$ released by IR measurements after combustion of the powdered sample. These measurements were performed in an alumina or a graphite crucible for the carbon and oxygen analyse, respectively. The calibration is achieved by steel standards containing well known carbon and oxygen contents.

In addition, the chemical composition of samples were locally analysed at the grain scale by electron microprobe (CAMECA SX 100, Gennevilliers, France) using a ZrO_2 standard and with a probe operating at 10 kV and 20 nA.

The oxycarbide powders were analysed by X-ray diffraction (D5000, Siemens AG, Munich, Germany) for angle (2θ) ranging between 20° and 120° (step: 0.03°, step time: 1.1 s) to identify the crystallized phases. From the XRD patterns, the lattice parameters were refined by Rietveld method.

Transmission electron microscopy (TEM) characterizations were carried out with a JEOL 2010 microscope (JEOL, Tokyo, Japan) operating at 200 kV to observe the morphology of synthesized oxycarbide powders. The specific areas of these powders were measured using the B.E.T. method (ASAP 2000, Micromeritics, Verneuil, France).

Concerning the SPS sintered samples, their final densities were determined by using the Archimedes method. Dynamic nanoindentation measurements (Young's modulus, Berkovich hardness) were made on mirror polished samples using a XP diamond nanoindenter (MTS Nano Instruments, Santa Clara, USA) with oscillations of 45 Hz and of 2 nm amplitude. Apparent elastic constants (Young's modulus, shear modulus) have been determined by ultrasonic method using 10 MHz transductors working in reflexion mode (WC37-10 and SW37-10, Ultran, State College, USA) on 5 mm thick samples. Finally, compressive creep tests have been carried out on fully dense samples using an INSTRON 8562 apparatus (INSTRON France SAS, Elancourt) equipped with silicon carbide pistons. Those experiments were performed at 1873 K under a vertical applied stress of 100 MPa and using flowing argon. In order to subtract the displacement of the two pistons, a LVDT displacement captor has been used to determine the exact instantaneous strain of the sample. Before being positioned in the assembly, the oxycarbide samples (3 mm × 3 mm × 8 mm) have been "mirror" polished and their edges have been chamfered in order to prevent cracking during the test.

3. Results and discussion

3.1. Chemical composition

Before studying the sintering behaviour of zirconium oxycarbide (ZrC_xO_y), it becomes critical to first characterize properly the chemical composition of the synthesized (Section 2.1) powders: oxygen content, structural and free carbon content.

The most common way to characterize the $x = O/Zr$ and $y = C/Zr$ ratios of a ZrC_xO_y composition consists in determining the lattice parameter of the oxycarbide phase by X-ray diffraction (XRD). Indeed, zirconium carbide ZrC_x exhibits a rock salt structure (*Fm*-3*m* space group) in which the oxygen could either be incorporated in the remaining vacant octahedral sites or be partly substituted to carbon. Then, the zirconium oxycarbide phase ZrC_xO_y adopts the same structure as zirconium carbide ZrC_x; but, the lattice parameter of the ZrC_xO_y phase is significantly modified by the incorporation of oxygen in the ZrC_x lattice.[10]

The XRD patterns of the synthesized powders (Fig. 1a) exhibit two groups. First, the four theoretical stoichiometries above $C/Zr \geq 0.80$ ($ZrC_{0.80}O_{0.20}$, $ZrC_{0.90}O_{0.10}$, $ZrC_{0.95}O_{0.05}$ and $ZrC_{1.00}$) are quite similar since all diffraction peaks of those powders represent a single-phased XRD pattern that can be indexed with the usual zirconium carbide data file (*e.g. Fm*-3*m*, JCPDS 00-035-0784); and so did not reveal the presence of residual zirconia in none of the samples. Conversely, the three other stoichiometries below $C/Zr \leq 0.70$ (*i.e.* $ZrC_{0.70}O_{0.30}$, $ZrC_{0.60}O_{0.40}$ and $ZrC_{0.50}O_{0.50}$) display some zirconia peaks in addition of those of ZrC_xO_y despite the fact that the reaction is completed. This proves that below $C/Zr = 0.80$, in the condition of temperature and atmosphere studied here, the zirconium oxycarbide phase is not reachable as a single phase, but imply two phases in thermodynamical equilibrium: ZrC_xO_y and ZrO_2.

Consequently, those specific synthesized powders (*i.e.* $C/Zr < 0.80$) will not be used in the continuation of the present study as the incorporation of an oxide would lead to the complete loss of specific refractory properties of zirconium (oxy)carbide.

The DRX patterns of the four studied stoichiometries (with $C/Zr \geq 0.80$) show a split of the $K_{\alpha 1}$ and $K_{\alpha 2}$ peaks which is observed since the low 2θ angles (Fig. 1b solely on two compositions for a better visualization). Such a splitting attests of the high chemical homogeneity of powders.[20] This property of high homogeneous chemical composition of the starting powders is a crucial parameter in the elaboration of monoliths in order to achieve high mechanical properties non-affected by the presence of chemical defects.

From Table 1, it also appears that the lattice parameter of samples decreases when increasing oxygen content. This is related to the displacement of the diffraction peaks toward the high diffraction angles (Fig. 1c) due to the progressive replacement of oxygen by carbon atoms in the zirconium carbide crystal lattice,[10,21] the radius of oxygen ($R_O = 0.66$ Å) being inferior to that of carbon ($R_C = 0.76$ Å).

TEM observations of the different zirconium oxycarbide powders with $C/Zr \leq 0.95$ (*i.e.* $ZrC_{0.80}O_{0.20}$, $ZrC_{0.90}O_{0.10}$ and $ZrC_{0.95}O_{0.05}$) did not reveal the presence of free carbon (Fig. 2a–c). That means the actual carbon content in these oxycarbide phases ($C/Zr \leq 0.95$) should not be too far in comparison with the theoretical stoichiometries. Conversely, TEM observation (Fig. 2d) of the powder with the highest starting carbon content $ZrC_{1.00}$ (theoretical composition) illustrates the presence of residual particles of amorphous free carbon (circled in white). These micrographs reveal also that the mean grain size of synthesized powders remains similar (≈0.5 μm) whatever the

Table 1
Main characteristics and chemical analyses of the different powdered and zirconium oxycarbide specimens.

Theoretical stoichiometry	Theoretical values			Elemental analysis (powder)			Calculated stoichiometry	Estimated C_{free} (wt.%)	Electron microprobe		BET	XRD
	O (wt.%)	C (wt.%)	Zr (wt.%)	O (wt.%)	C (wt.%)	Calculated Zr (wt.%)			Powder O (wt.%)	Monolith O (wt.%)	Specific area ($m^2\ g^{-1}$) (±0.05)	Lattice parameter (Å) (±0.001)
$ZrC_{1.00}$	0.00	11.63	88.37	0.69 ± 0.04	11.23 ± 0.05	88.08	$ZrC_{0.97}O_{0.04}$ $ZrC_{0.96}O_{0.04}$*	0.2	0.70 ± 0.03	0.77 ± 0.05	1.40	4.698
$ZrC_{0.95}O_{0.05}$	0.77	11.03	88.20	0.72 ± 0.05	10.90 ± 0.03	88.38	$ZrC_{0.94}O_{0.05}$	0	0.83 ± 0.05	0.79 ± 0.04	1.15	4.695
$ZrC_{0.90}O_{0.10}$	1.54	10.43	88.03	1.11 ± 0.07	10.37 ± 0.03	88.52	$ZrC_{0.89}O_{0.07}$	0	1.13 ± 0.09	1.12 ± 0.20	1.15	4.688
$ZrC_{0.80}O_{0.20}$	3.08	9.24	87.69	2.01 ± 0.10	9.24 ± 0.04	88.75	$ZrC_{0.79}O_{0.13}$	0	2.12 ± 0.35	2.19 ± 0.31	1.12	4.680
$ZrC_{0.70}O_{0.30}$	4.60	8.05	87.35	2.70 ± 0.13	8.47 ± 0.05	88.83		0				4.679 + ZrO_2
$ZrC_{0.60}O_{0.40}$	6.10	6.87	87.02	3.69 ± 0.15	7.56 ± 0.10	88.75		0				4.679 + ZrO_2
$ZrC_{0.50}O_{0.50}$	7.60	5.71	86.69	5.54 ± 0.07	6.74 ± 0.04	87.72		0				4.679 + ZrO_2

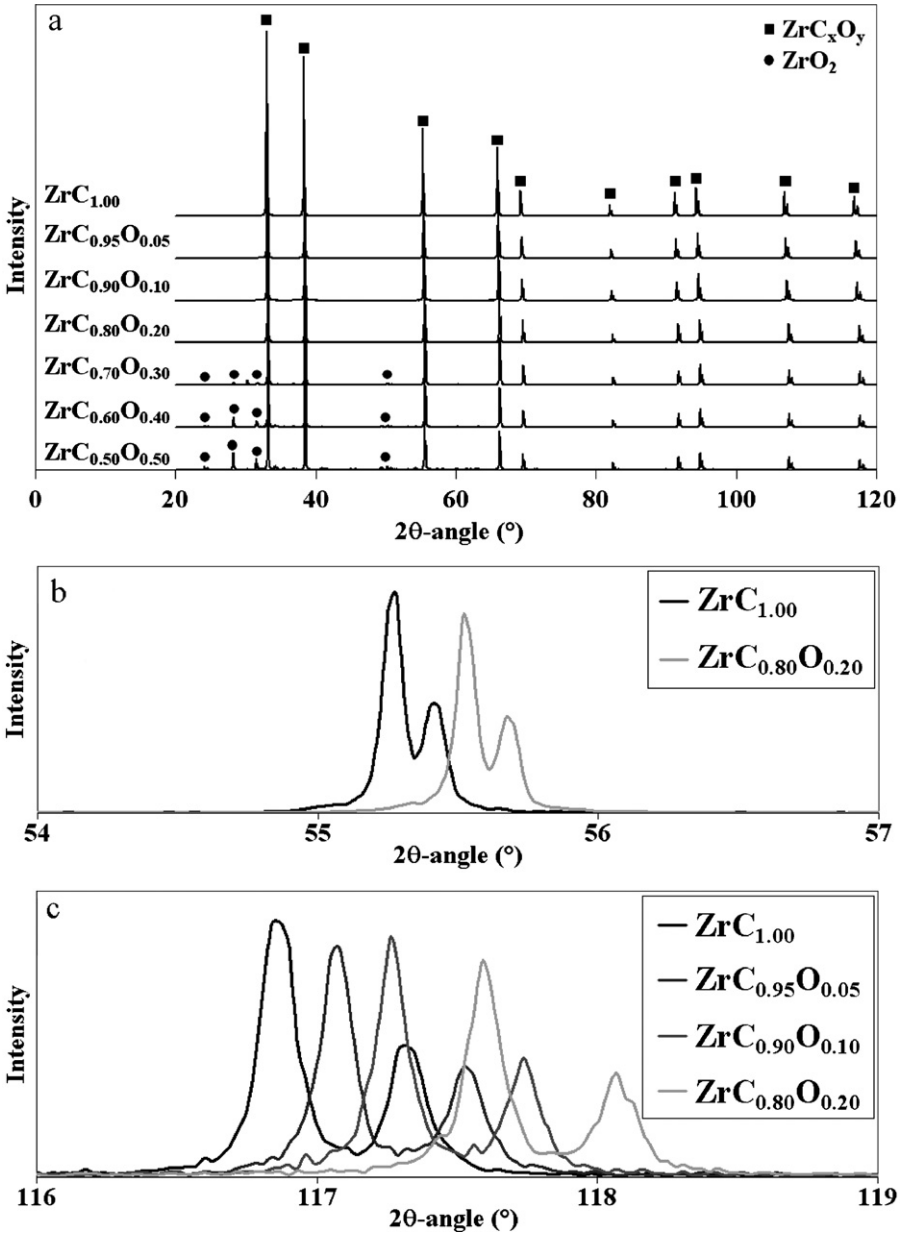

Fig. 1. (a) X-ray diffraction patterns from 20° to 120° of synthesized powders with different theoretical compositions. (b) Focus of diffraction peaks between 54° and 57° (reflexion 220) for $ZrC_{0.80}O_{0.20}$ and $ZrC_{1.00}$. (c) Focus of diffraction peaks between 116° and 119° (reflexion 511) for $ZrC_{0.80}O_{0.20}$, $ZrC_{0.90}O_{0.10}$, $ZrC_{0.95}O_{0.05}$ and $ZrC_{1.00}$.

target composition. Consequently, the difference encountered between the values of specific area for powders with C/Zr ≤ 0.95 (≈1.15 $m^2\,g^{-1}$) and $ZrC_{1.00}$ (1.40 $m^2\,g^{-1}$) confirms the presence of free carbon in the $ZrC_{1.00}$ powder. Indeed, free carbon displays higher specific area (>30 $m^2\,g^{-1}$) which could significantly modify the specific area of the carboreduction products.

To define accurately the chemical composition of the ZrC_xO_y phase, the powdered samples have been analysed globally by elemental analysis and locally by electron microprobe. The main results have been reported in Table 1. The zirconium content has been estimated both from oxygen and carbon contents and by considering the mass conservation for a ZrC_xO_y composition.

XRD and TEM experiments have shown that no residual zirconia reactant was present within all the final powders. Consequently, it can be supposed that the measured oxygen content reported in Table 1 should only be relevant to the oxygen incorporated in the zirconium oxycarbide crystal lattice. It is shown that a good agreement is observed between the measured oxygen stoichiometry and the theoretical one. From Table 1, it appears that the oxygen contents, determined for a theoretical stoichiometry of the oxycarbide phase, tend to be similar whatever the analytical method used. The fact that the oxygen content is equivalent at local (*i.e.* grain) and global (*i.e.* powder) scale confirms the chemical homogeneity of the sample previously suggested by XRD patterns.

From elemental chemical analysis, overall amount of carbon was determined involving the contribution of both structural carbon incorporated within the oxycarbide lattice and the even-

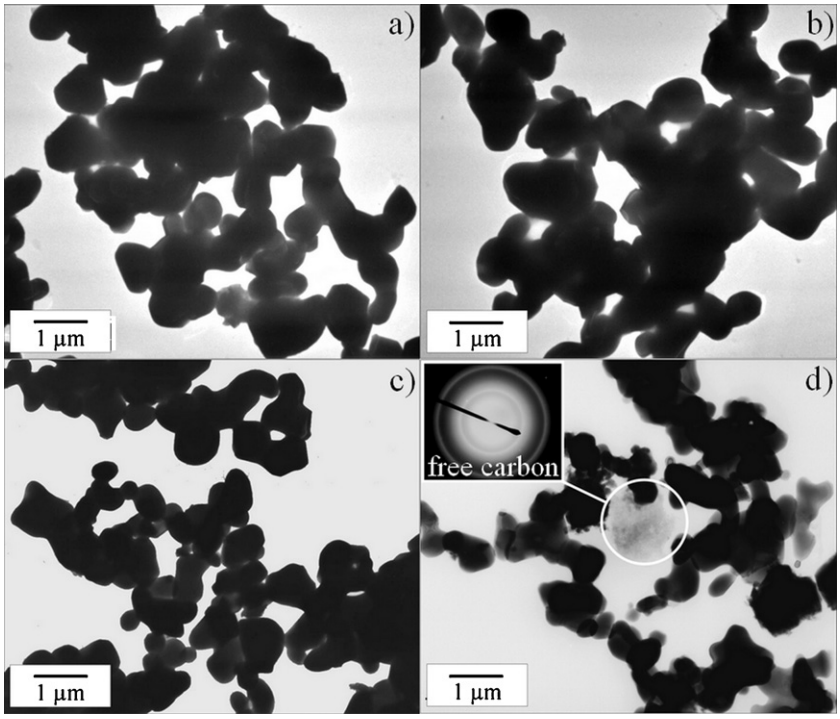

Fig. 2. TEM micrographs of (a) $ZrC_{0.80}O_{0.20}$, (b) $ZrC_{0.90}O_{0.10}$, (c) $ZrC_{0.95}O_{0.05}$ and (d) $ZrC_{1.00}$ powders, residual free carbon particle is circled in white.

tual occurrence of unreacted free carbon. On the one hand, as previously demonstrated, when the analysed sum C/Zr + O/Zr remained inferior to 1 (*i.e.* $C/Zr_{theo} \leq 0.95$), TEM observations attested that no residual free carbon was present. This result reveals that the carbon content measured by elemental analysis strictly corresponds to structural carbon. On the other hand, in the case of the $ZrC_{1.00}$ sample, the occurrence of free carbon (Fig. 2b) would correspond to the carbon content which would not be integrated within the oxycarbide lattice. In these conditions, the sum C/Zr + O/Zr (*i.e.* $x + y$) would be superior to 1 leading to an oxycarbide phase with an overstoichiometric composition close to $ZrC_{0.97}O_{0.04}$. This latter could be corrected as $ZrC_{0.96}O_{0.04}$* (Table 1) to obtain a saturated lattice ZrC_xO_{1-x} for the same powder. Consequently, the free carbon content which could be considered as the carbon content in overstoichiometry (*i.e.* 1 − (C/Zr + O/Zr)) should be around 0.2 wt.% for the $ZrC_{1.00}$ theoretical composition. This free carbon content would correspond to a significant amount of 1 vol.%. According to previous works[22], the presence of residual free carbon in the starting zirconium (oxy)carbide powders should be related to the appearance of graphite intergranular inclusions after their SPS treatment. These inclusions could lead to a decrease of the mechanical performances of ZrC-based materials and, more generally, of the transition metal carbides by favoring the microcracks displacement along the graphite planes.[7,22–24]

It is thus important to notice that the discrepancy with the lattice saturated stoichiometry (*i.e.* O/Zr + C/Zr < 1) seems to increase when increasing the oxygen content. This phenomenon must be related to the probable stabilization of lattice carbon vacancies in the oxycarbide crystal as reported in the literature for others substoichiometric transition metal carbides (MC_x with $x < 1$).[15,25,26] More particular, the crossed substitution of carbon atoms by oxygen in the zirconium carbide lattice could lead to the stabilization of a higher density of vacancies.

From these observations, it appears that the experimental protocol used to synthesise ZrC_xO_y can lead to a fine powder with homogeneous and controlled carbon and oxygen contents. Moreover, these results demonstrated that it would be necessary to target a minimal oxygen content (*e.g.* C/Zr = 0.95) to avoid free carbon but keeping a high structural carbon content in the powders.

Finally, the theoretical stoichiometries of the oxycarbide phase evidencing no free carbon will be studied in the continuation of this article and will be replaced by their respective actual stoichiometries determined chemical analyses:

$$ZrC_{0.95}O_{0.05} \rightarrow ZrC_{0.94}O_{0.05},$$
$$ZrC_{0.90}O_{0.10} \rightarrow ZrC_{0.89}O_{0.07}$$
$$\text{and } ZrC_{0.80}O_{0.20} \rightarrow ZrC_{0.79}O_{0.13}.$$

3.2. Sintering behaviour

The densification behaviour of three stoichiometries of zirconium oxycarbide ($ZrC_{0.94}O_{0.05}$, $ZrC_{0.89}O_{0.07}$ and $ZrC_{0.79}O_{0.13}$) has been compared under the same SPS conditions: 100 K/min up to 2460 K under 50 MPa with a dwell of 5 min. The thermal cycle is described in detail in Fig. 3. It is important to remind that all these powders present a similar average grain size (≈0.5 µm) and negligible free carbon content.

Before studying the densification kinetics, it can be noticed in the Table 1 that electron microprobe analyses do not show

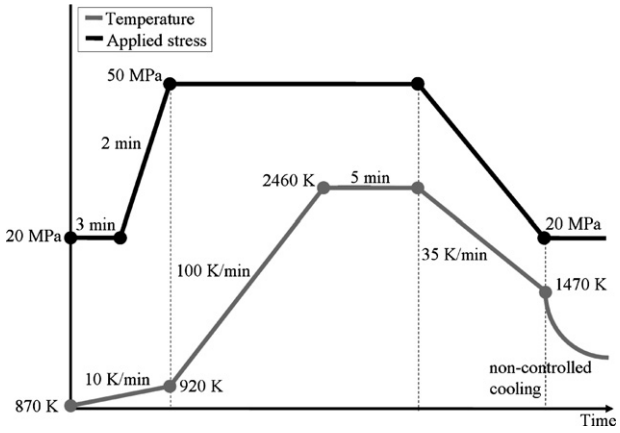

Fig. 3. Schematic representation of temperature and applied stress cycles during SPS treatment.

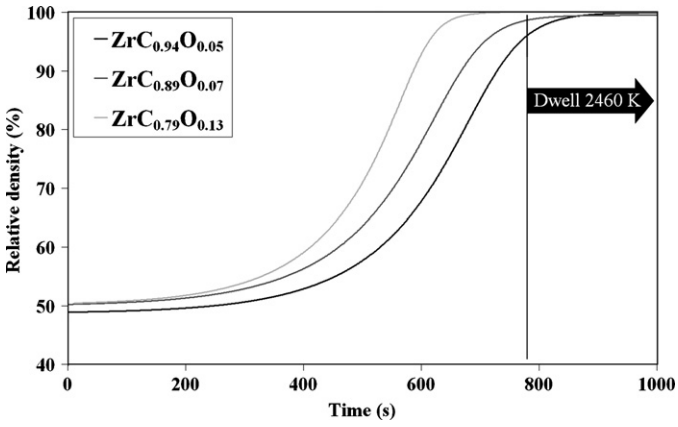

Fig. 5. Relative density as a function of time for $ZrC_{0.94}O_{0.05}$, $ZrC_{0.89}O_{0.07}$ and $ZrC_{0.79}O_{0.13}$ powders (100 K/min, 2460 K, 50 MPa).

any significant evolution of the oxygen content after sintering. This result attests of the chemical stability of the different stoichiometries of synthesised powders even under a severe thermal treatment.

Concerning the spark plasma sintering treatment, the densification rate $[(1/\rho)(d\rho/dt)]$ as a function of the corrected temperature is reported in Fig. 4. From this latter, it appears that the temperature of the shrinkage beginning strongly depends on the composition of the oxycarbide phase. So, the densification seems to begin around 1600 K for $ZrC_{0.79}O_{0.13}$, whereas for the lowest oxygen content oxycarbide (*i.e.* $ZrC_{0.94}O_{0.05}$) the densification shifts to the higher temperature (*i.e.* 1700 K). In the same manner, the densification rate reaches its maximum at 2100 K for $ZrC_{0.79}O_{0.13}$ as opposed to 2300 K for $ZrC_{0.94}O_{0.05}$. As a consequence, the soaking time needed to achieve full dense samples is shorter for oxycarbide powders containing high oxygen content (Fig. 5). As an example, the $ZrC_{0.79}O_{0.13}$ sample is fully sintered from 1 min before the start of the dwell, whereas the $ZrC_{0.94}O_{0.05}$ sample requires a dwell of 5 min at 2460 K to reach its theoretical density. SEM observations of specimens treated 2 min at 2460 K (Fig. 6a and b) confirm the significant effect of stoichiometry on the sintering kinetics. Indeed, the average grain size of sintered $ZrC_{0.79}O_{0.13}$ (2.5 μm) specimens appears to be at least two times higher than the one obtained in the same conditions for the $ZrC_{0.94}O_{0.05}$ sample (1 μm). This more important grain growth observed for the highest oxygen content could be explained by considering two main causes: an enhanced diffusion kinetic and an earlier beginning of the final stage of sintering.

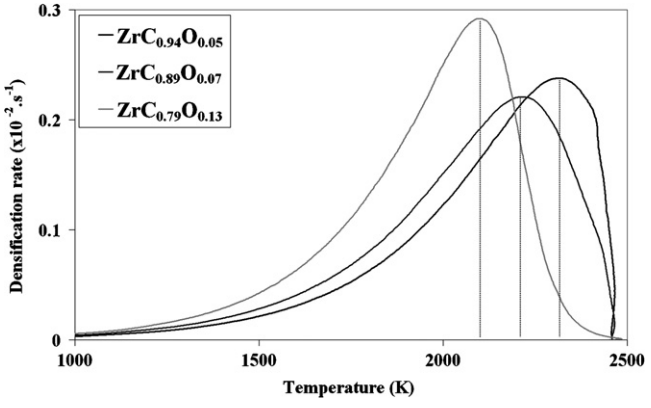

Fig. 4. Densification rate as a function of temperature for $ZrC_{0.94}O_{0.05}$, $ZrC_{0.89}O_{0.07}$ and $ZrC_{0.79}O_{0.13}$ powders (100 K/min, 2460 K, 50 MPa).

Finally, the increase of the oxygen content in zirconium oxycarbide enhances the densification kinetics during isothermal or non-isothermal SPS treatment. A similar influence has been reported by Barnier et al.[14] during hot-pressing of zirconium oxycarbide powders. This phenomenon could be principally explained by two factors. First, the incorporation of oxygen in the ZrC crystal lattice would weaken the covalent character of the Zr–C bounding in favour of the more ionic character of the Zr–O bounding and would increase the sinterability of this ceramic by promoting the species mobility during the thermal treatment.

Secondly, from the results obtained during this study, it has been highlighted that the amount of lattice vacancies increases together with the oxygen content. In the crystal lattice, this increase of the vacancies density would enhance the mass transport by diffusion of atoms and, consequently, the densification and the grain growth processes.

3.3. Mechanical properties

In order to approach the effect of the chemical composition of zirconium oxycarbide phase on the mechanical properties at room temperature, ultrasonic measurements and dynamic nanoindentation experiments have been carried out for the two extreme compositions of SPS sintered specimens. More particular, the corresponding compositions and sintering conditions are: $ZrC_{0.94}O_{0.05}$ (5 min at 2460 K under 50 MPa, $\varnothing_m \approx 4.7$ μm) and $ZrC_{0.79}O_{0.13}$ (2 min at 2460 K under 100 MPa, $\varnothing_m \approx 5.2$ μm). These sintering conditions have been retained since they provide full dense samples with an equivalent average grain size close to 5 μm.

First, it can be noticed that the ultrasonic measurements and nanoindentation experiments could be considered as complementary tests. Indeed, the dynamic nanoindentation method provides to the intrinsic mechanical properties of ceramics such as Young's modulus or Berkovich hardness. In this latter case,

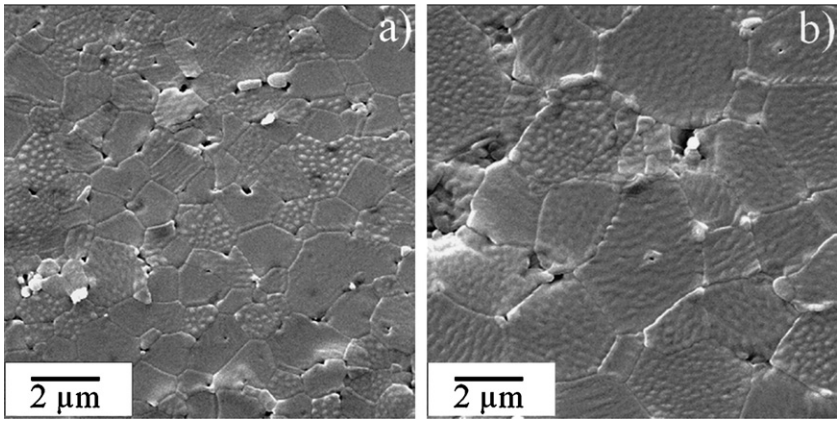

Fig. 6. SEM micrographs presenting microstructures of sintered $ZrC_{0.94}O_{0.05}$ (a) and $ZrC_{0.79}O_{0.13}$ (b) (2460 K, 2 min, 50 MPa).

the using of a nanosized diamond probe rests on the mechanical response of a single grain and thus avoids the influence of grain boundaries or intergranular inclusions. Conversely, ultrasonic measurements allow determining the apparent elastic constants such as Young's or shear modulus of the ceramics, and so, taking account of the microstructural features of the sintered samples (porosity, grain size, grain boundaries and intergranular secondary phases). The main mechanical properties so-obtained at room temperature are reported in Table 2.

From the dynamic nanoindentation results, it can be noticed that the intrinsic properties would deeply depend on the chemical composition of the zirconium oxycarbide. Both Young's modulus and Berkovich hardness are enhanced with the structural carbon amount; and so the $ZrC_{0.94}O_{0.05}$ compound shows values respectively 15% and 35% higher compared to the $ZrC_{0.79}O_{0.13}$ sintered specimen. The same trend is observed when the apparent elastic properties are determined by ultrasonic measurements: $ZrC_{0.94}O_{0.05}$ sintered sample exhibits values of Young's and shear moduli which are 10% higher than the sample showing higher oxygen content.

Furthermore, the apparent and the intrinsic Young's moduli appear to be very close whatever the chemical composition of the oxycarbide phase, meaning that the mechanical properties of SPS sintered samples are rather governed by the structural properties of the oxycarbide phase than by their microstructural features. These analogous values also suggest that the grain boundaries would be free of any porosity or free carbon impurities.

It is thus important to notice that mechanical properties of the $ZrC_{0.94}O_{0.05}$ composition are similar and often better than the values reported for a given ZrC composition in the literature.[1,7,10,24]

This could appear in contradiction with the influence of oxygen content reported in this study. Nevertheless, the actual composition of zirconium (oxy)carbide is often neglected or is not accurately determined in the previous works. In particular, when commercial powders are used, the reported oxygen content and the free carbon amount can reach 0.5–1 wt.% and 1–1.5 wt.% respectively.[1,6,7,10,22] As a matter of fact, the intrinsic properties of $ZrC_{0.94}O_{0.05}$ are similar to the values reported in literature (*e.g.* $E = 464 \pm 22$ GPa, $H = 25.2 \pm 1.4$ GPa found by Sciti et al.[7] by nanoindentation). In the same way, the present apparent properties of the $ZrC_{0.94}O_{0.05}$ specimen are classically higher than the values reported in literature (*i.e.* Young's modulus values ranging around 390–400 GPa[1,10,24]), what suggests the presence of secondary phases in these latter samples.

Nevertheless, even if the prevailing results show a significant influence of the chemical composition on the mechanical properties of ZrC_xO_y, the obtained values in the studied range of stoichiometry ($ZrC_{0.79}O_{0.13}$ to $ZrC_{0.94}O_{0.05}$) remains high enough to consider that the zirconium oxycarbide can be used as a structural material at room temperature and whatever its composition.

However, as mentioned in the introduction, the main advantage of zirconium (oxy)carbide is its high refractarity. Thus, in order to evaluate the effect of the chemical composition of ZrC_xO_y on its mechanical resistance at high temperature, compressive creep tests have been conducted at 1873 K under a 100 MPa vertical applied stress on the same samples as reported in the previous paragraph. This type of experiment is essential in order to evaluate the ability of a structural material to resist in severe conditions of use.

Fig. 7 exhibits for each of the two tested compositions the evolution of strain $\varepsilon = (\Delta L/L) = (\Delta L/(L_0 - \Delta L))$ during the

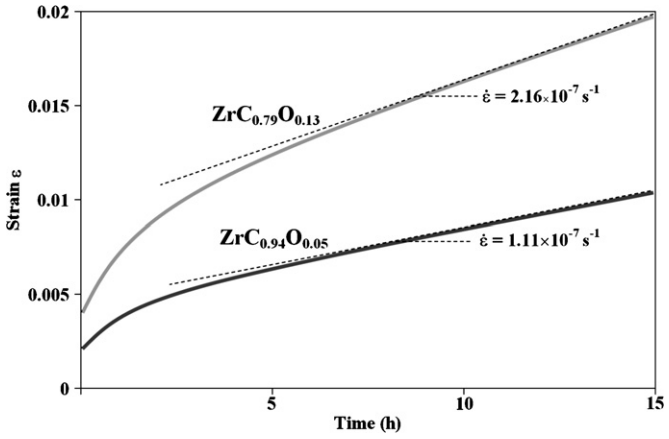

Fig. 7. Evolution of instantaneous strain as a function of time during compressive creep tests at 1873 K under 100 MPa for $ZrC_{0.94}O_{0.05}$ and $ZrC_{0.79}O_{0.13}$ dense samples.

Table 2
Main mechanical properties of $ZrC_{0.94}O_{0.05}$ and $ZrC_{0.79}O_{0.13}$ dense samples.

Stoichiometry	Average grain size (μm)	Porosity (%)	Ultrasonic measurements		Dynamic nanoindentation	
			Apparent shear modulus (GPa)	Apparent Young's modulus (GPa)	Intrinsic Young's modulus (GPa)	Berkovich hardness (GPa)
$ZrC_{0.94}O_{0.05}$	4.7 ± 0.2	<1	173 ± 5	420 ± 6	441 ± 10	28.3 ± 1.0
$ZrC_{0.79}O_{0.13}$	5.2 ± 0.2	<1	156 ± 6	380 ± 7	383 ± 13	21.0 ± 1.4

experiments (with L_0 and L the initial and instantaneous length, respectively). From these results, after approximately 7 h, the steady state is achieved for both compositions as shown by the constant creep rates $\dot{\varepsilon} = d\varepsilon/dt$. According to the values of creep rate during steady state, the chemical composition of the oxycarbide seems to have a significant effect on the creep resistance. Indeed, the $ZrC_{0.94}O_{0.05}$ sample exhibits a creep rate ($\dot{\varepsilon} = 1.11 \times 10^{-7}\,s^{-1}$) which is twice slower than the one of $ZrC_{0.79}O_{0.13}$ sample ($\dot{\varepsilon} = 2.16 \times 10^{-7}\,s^{-1}$). As a matter of fact, the creep resistance is drastically weakened by the reduction of structural carbon content in the oxycarbide stoichiometry. Finally, only the $ZrC_{0.94}O_{0.05}$ composition could maintain the refractory properties of zirconium carbide by exhibiting a creep resistance close that reported for $ZrC_{0.97}$ by Zubarev et al.[27] This highlights the fact that the oxygen content should be necessarily minimized in the ZrC_xO_y stoichiometry in order to use zirconium oxycarbide for high temperature applications.

In the same manner that we have explained the improvement of sintering kinetics (Section 2), this deterioration of mechanical properties can be attributed both to the proportion of oxygen and vacancies in the oxycarbide ZrC_xO_y. Indeed, when decreasing the C/Zr ratio, the variation of composition is traduced by the progressive replacement of strong covalent bonds (Zr–C) by metallic (Zr–Zr) and ionic (Zr–O) bonds. As a consequence, the mechanical properties could be altered at room temperature principally by a weaker average strength of bonds, and at high temperature mainly by a lattice diffusion promoted by the presence of a higher density of vacancies in the $ZrC_{0.79}O_{0.13}$ composition.

4. Conclusion

The present study proves the possibility to synthesise micro-sized zirconium oxycarbide powders with controlled stoichiometries and avoiding the presence of impurities. Electron microprobe and DRX experiments confirm the high chemical homogeneity of the synthesised powders. From the stability domain of ZrC_xO_y phase, the increase of O/Zr ratio leads to the stabilization of a significant amount of carbon vacancies in the zirconium oxycarbide crystal lattice.

Otherwise, the incorporation of oxygen in the zirconium carbide lattice leads to both a significant enhancement of the densification kinetics during spark plasma sintering treatment and an important decrease of mechanical properties at room and at high temperature; by promoting the formation of further carbon vacancies and by weakening the initial boundings in the crystal lattice. Nevertheless, the mechanical properties of the most refractory synthesized composition $ZrC_{0.94}O_{0.05}$, allow considering this SPS sintered material as a serious candidate for thermostructural applications.

Acknowledgements

The authors wish to thank Claude Estournès, Geoffroy Chevallier and Gwénaëlle Raimbeaux for the SPS experiments,

Yohann Ravaux for the electron microprobe analyses and Sarah Deniel for nanoindentations experiments.

References

1. Toth LE. *Transition Metal Carbides Nitrides*. New York, London: Academic Press; 1971.
2. Gosset D, Dollé M, Simeone D, Baldinozzi G, Thomé L. Structural behaviour of nearly stoichiometric ZrC under ion irradiation. *Nucl Instrum Methods Phys Res Sect B* 2008;**266**:2801–5.
3. Bulychev VP, Andrievskii RA, Nezhevenko LB. Theory and technology of sintering, thermal, and chemicothermal treatment processes. *Powder Metall Met Ceram* 1977;**16**:273–6.
4. Min-Haga E, Scott WD. Sintering and mechanical properties of ZrC–ZrO_2 composites. *J Mater Sci* 1988;**23**:2865–70.
5. Kim KH, Shim KB. The effect of lanthanum on the fabrication of ZrB_2–ZrC composites by spark plasma sintering. *Mater Char* 2003;**50**: 31–7.
6. Silvestroni L, Sciti D. Microstructure and properties of pressureless sintered ZrC-based materials. *J Mater Res* 2008;**23**:1882–9.
7. Sciti D, Guicciardi S, Nygren M. Spark plasma sintering and mechanical behaviour of ZrC-based composites. *Scr Mater* 2008;**59**:638–41.
8. Allemand A, Le Flem (Dormeval) M, Guillard F. Sintering of ZrC by hot isostatic pressing (HIP) and spark plasma sintering (SPS); effect of impurities. In: *Proceedings of "Sintering 2005"*. 2005. p. 176–9.
9. Orrù R, Licheri R, Loccic AM, Cincotti A, Cao G. Consolidation/synthesis of materials by electric current activated/assisted sintering. *Mater Sci Eng R* 2009;**63**:127–287.
10. Storms EK. *The Refractory Carbides*. New York, London: Academic Press; 1967.
11. Constant K, Kieffer R, Ettmayer P. Über das pseudoternäre System "ZrO"–ZrN–ZrC. *Monatsh Chem* 1975;**106**:823–32.
12. Ouensanga AH, Dodé M. Etude thermodynamique et structurale a haute température du système Zr–C–O Diagramme de phases a 1555 °C. *J Nucl Mater* 1976;**59**:49–60.
13. Samsonov GV. Imperfection of carbon sublattice: effect on the properties of refractory carbides of transition metals. *Powder Metall Met Ceram* 2008;**47**:13–20.
14. Barnier P, Thévenot F. Synthesis and hot-pressing of single-phase ZrC_xO_y and two-phase ZrC_xO_y–ZrO_2 materials. *Int J High Technol Ceram* 1986;**2**:291–307.
15. Ouensanga AH, Dodé M. Study of oxygen solubility in zirconium carbide at 1555 °C with free carbon and in thermodynamical equilibrium conditions. *Rev Int Htes Temp Et Réfract* 1974;**11**:35–9.
16. Leprince-Ringuet F, Lejus AM, Collongues R. Preparation and fusion in a plasma furnace of refractory carbides, nitrides and oxynitrides. *Compt Rend Acad Sci Fr* 1964;**258**:221–3.
17. Maître A, Lefort P. Solid state reaction of zirconia with carbon. *Solid State Ionics* 1997;**104**:109–22.
18. Gendre M, Maître A, Trolliard G. A study of the densification mechanisms during spark plasma sintering of zirconium (oxy-)carbide powders. *Acta Mater* 2010;**58**:2598–609.
19. Antou G, Gendre M, Trolliard G, Maître A. Spark plasma sintering of zirconium carbide and oxycarbide: finite element modeling of current density, temperature, and stress distributions. *J Mater Res* 2009;**24**:404–12.
20. Rempel' AA, Raichenko AI. Preparation of disordered and ordered highly nonstoichiometric carbides and evaluation of their homogeneity. *Phys Solid State* 2000;**42**:1280–6.
21. Cruz Fernandes J, Amaral PM, Guerra Rosa L. X-ray diffraction characterisation of carbide and carbonitride of Ti and Zr prepared through reaction between metal powders and carbon powders (graphitic or amorphous) in a solar furnace. *Int J Refract Met Hard Mater* 1999;**17**:437–43.
22. Goutier F, Trolliard G, Maître A, Valette S, Estournès C. Role of the impurities on the SPS sintering of ZrC–ZrB_2 composites. *J Eur Ceram Soc* 2008;**28**:671–8.
23. Kreimer GS, Vakhovskaya MR. The effect of carbon content on the mechanical properties of tungsten carbide–cobalt hard alloys. *Powder Metall Met Ceram* 1965;**4**:454–9.
24. Kral C, Lengauer W, Rafaja D, Ettmayer P. Critical review on the elastic properties of transition metal carbides, nitrides and carbonitrides. *J Alloys Compd* 1998;**265**:215–33.
25. Larin AA, Vlasov VG. Effect of oxygen content on the structural characteristics of uranium oxycarbides. *Powder Metall Met Ceram* 1974;**13**:761–3.
26. Sarkar SK, Miller AD, Mueller JI. Solubility of oxygen in ZrC. *J Am Ceram Soc* 1972;**55**:628–30.
27. Zubarev PV, Dement'ev LN. Relation between the activation energies of high-temperature creep and diffusion in transition metal carbides. *Strength Mater* 1971;**3**:1058–61.